



ELSEVIER

The analysis of “empty space” in the PdGa<sub>5</sub> structureYuri Grin<sup>a,\*</sup>, Ulrich Wedig<sup>a</sup>, Frank Wagner<sup>a</sup>, Hans Georg von Schnering<sup>a</sup>, Andreas Savin<sup>b</sup><sup>a</sup>Max-Planck-Institut für Festkörperforschung, Heisenbergstraße 1, D-70569 Stuttgart, Germany<sup>b</sup>Laboratoire de Chimie Théorique, Université Pierre et Marie Curie, 4 Place Jussieu, 75252 Paris cédex, France

Received 17 September 1996

## Abstract

The structure of PdGa<sub>5</sub> is characterized by a framework of condensed bicapped tetragonal antiprisms [PdGa<sub>10</sub>]. The appropriate symmetry governed periodic nodal surface (PNS) divides the space into two labyrinths. The atoms of the coordination polyhedra are located in one labyrinth or are close to the surface. The second labyrinth seems to be “empty”. The electron localization function (ELF) calculated by the TB-LMTO method, shows that the “empty” labyrinth contains the regions with high ELF values. These regions are related to inter-polyhedral Ga–Ga bonds forming Ga<sub>4</sub> squares. The vertices of eight covalently bonded Ga<sub>4</sub> squares build tetragonal antiprisms which are centered by Pd atoms. High electron density but low ELF values inside these coordination polyhedra of Pd represent regions of delocalized (metal-like) electrons. Thus, the PNS separates the regions of different bonding character. Some relations to stuffed derivatives of the PdGa<sub>5</sub> structure are discussed.

## 1. Introduction

The structures of a series of binary transition metal compounds MN<sub>x</sub> ( $x > 2$ ) with elements E13, E14 and E15 as majority components N, have been analyzed with the help of periodic nodal surfaces (PNS) [1], as well as the electron localization function (ELF) [2]. In general, these structures are characterized by exclusively heteroatomic coordination of the M atoms (CN 8–10), whereas the coordination of the N atoms is homoatomic as well. The ratio of the interatomic distances falls into the range  $1.15 < d(N-N)/d(M-N) < 1.35$  as a necessary consequence of the stoichiometric ratio  $x > 2$  and the large coordination number of the M atoms. Therefore, the distances  $d(N-N)$  are in the range of covalent bonds (bond order about 1/2) and it is an important question, whether there are direct N–N interactions or not.

Very recently, the structure of RhBi<sub>4</sub> was described as the first representative of this series [3]. It was shown that the two enantiomorphic frameworks of condensed RhBi<sub>8</sub> tetragonal antiprisms are enveloped by the appropriate PNS and that the “empty” labyrinth, which separates the two frameworks, represents a hyperbolic lone pair layer structure.

2. The crystal structure of PdGa<sub>5</sub>

The structure of PdGa<sub>5</sub> is represented in Fig. 1(a) in the classical way. The structural data are taken from [4]: space group *I4/mcm*,  $a = 6.436(6)$ ,  $c = 9.990(8)$  Å,  $c/a = 1.552$ ,  $Z = 4$ . The tetragonal *I4/mcm* structure is a three-dimensional system of condensed bicapped tetragonal antiprisms  ${}^3[\text{PdGa}_{10/2}^{\text{cap}}]$ . One can formally distinguish between columns along [001] with condensation via common corners and layers parallel (001) with condensation via common edges. Eight Ga1 atoms form the tetragonal antiprismatic fragment of the coordination polyhedron around the Pd atom. Two Ga2 atoms cap this fragment along [001], forming one-dimensional  ${}^1_2[\text{Pd}_2\text{Ga}_2]$  chains. The important interatomic “intra-cluster” distances are:  $d(\text{Pd-Ga}) = 2.496$  Å ( $2 \times \text{Ga}_2$ ), 2.697 Å ( $8 \times \text{Ga}_1$ );  $d(\text{Ga}_1\text{-Ga}) = 2.828$  Å ( $8 \times \text{Ga}_2$ ), 2.898 Å ( $4 \times \text{Ga}_1$ ), 2.903 Å ( $4 \times \text{Ga}_1$ ), 3.480 Å ( $8 \times \text{Ga}_1$ ). The average values are  $\bar{d}(\text{Pd-Ga}) = 2.657$  Å and  $\bar{d}(\text{Ga-Ga}) = 3.070$  Å with the ratio  $\bar{d}(\text{Ga-Ga})/\bar{d}(\text{Pd-Ga}) = 1.16$ . The shortest “inter-cluster” distances are in the Ga<sub>4</sub> squares (see below):  $d(\text{Ga}_1\text{-Ga}_1) = 2.669$  and 2.787 Å, respectively.

3. Periodic nodal surface in the PdGa<sub>5</sub> structure

The periodic nodal surface was calculated according to von Schnering and Nesper [5] with the Fourier series:

\*Corresponding author.

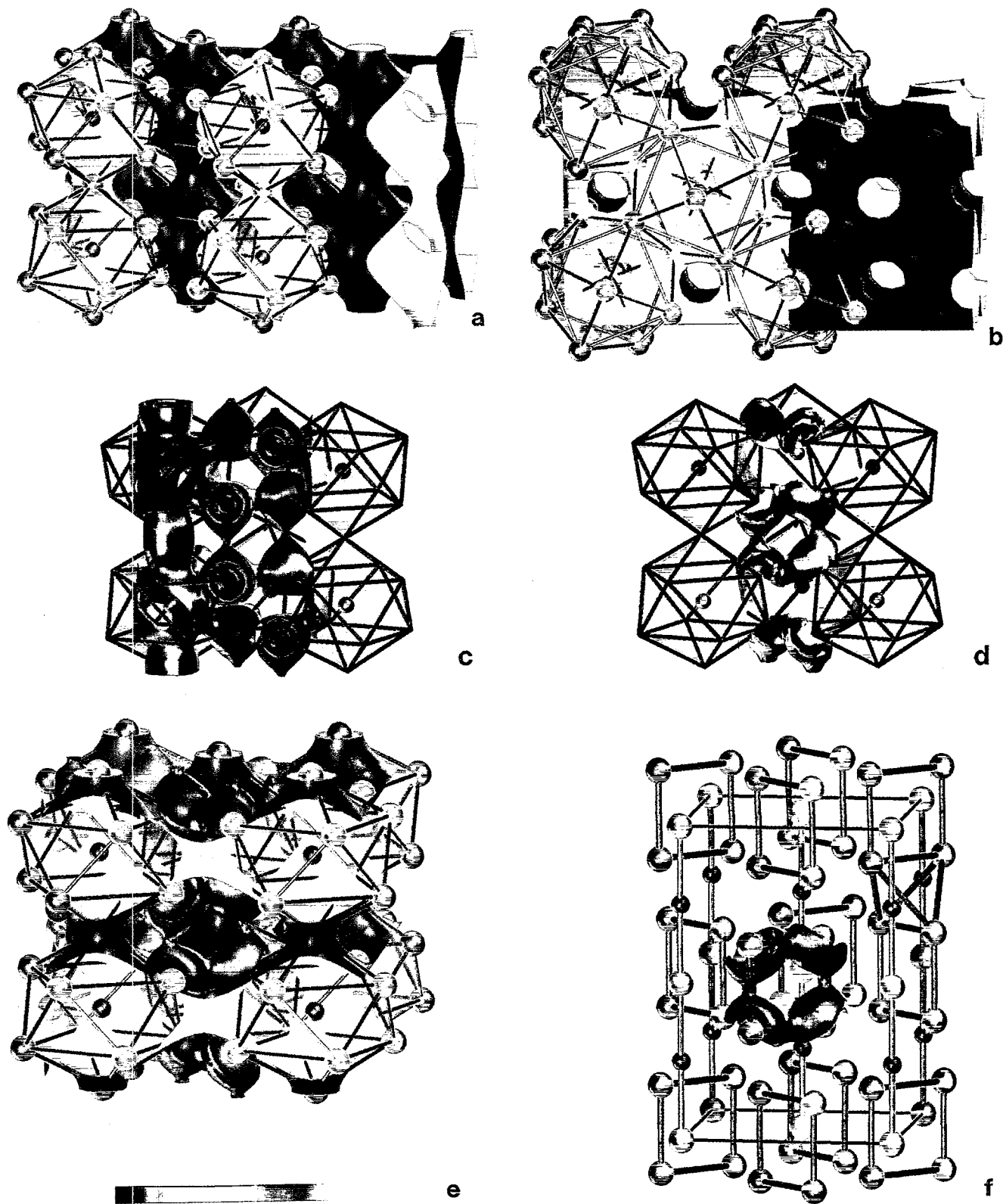


Fig. 1. (a) The structure of PdGa<sub>5</sub> as a framework of bicapped tetragonal antiprisms [PdGa<sub>10</sub>] together with the periodic nodal surface, PNS (blue; see text). View approximately along [100]. Pd=red spheres, Ga=green spheres. (b) View approximately along [001]. (c) The electron density isosurface  $p = 0.035 \text{ e}^-/\text{a.u.}^3$  (blue). (d) The electron localization function isosurface  $\text{ELF} = 0.65$  (red). (e) Regions with  $\text{ELF} > 0.65$  (red clouds) embedded in the "empty" labyrinth of the PNS. (f) Covalently bonded Ga<sub>4</sub> squares (black) with the isosurface  $\text{ELF} = 0.65$  of the valence electrons (red) and the Pd-Ga<sub>2</sub>-chains (blue) along [001].

$$R(\mathbf{r}) = \sum_{\mathbf{h}} [|S(\mathbf{h})| k_{\mathbf{h}} \cos(2\pi \mathbf{h} \cdot \mathbf{r} - \alpha(\mathbf{h}))] = 0.$$

$S(\mathbf{h}) = \sum_i \delta_i \exp(2\pi i \mathbf{h} \cdot \mathbf{r}_i)$  is the geometric structure factor;  $k_{\mathbf{h}} = (|\Phi_{\mathbf{h}}|/|\mathbf{h}|)^2$  is a decay function;  $\mathbf{h}$  and  $\mathbf{r}$  are the vectors in reciprocal and direct space,  $\mathbf{h} = h\mathbf{a}^* + k\mathbf{b}^* + l\mathbf{c}^*$  (in short form  $\mathbf{h} = ha$ ) and  $\mathbf{r} = x\mathbf{a} + y\mathbf{b} + z\mathbf{c}$  (in short form  $\mathbf{r} = xa$ ) respectively;  $\alpha(\mathbf{h})$  is the symmetry related phase shift of  $S(\mathbf{h})$ .

The space group  $I4/mcm$  of  $\text{PdGa}_5$  and the unit cell dimensions show that the general pattern of four formula units should be strongly related to a simple cubic one. The matrix  $(\frac{1}{2}, \frac{1}{2}, 0; -\frac{1}{2}, \frac{1}{2}, 0; 0, 0, \frac{1}{2})$  transforms the tetragonal unit cell into the quasi cubic one ( $c/a = 1.098$ ), showing directly the relation to the structure types of  $\text{CsCl}$ ,  $\text{ReO}_3$  and  $\text{CaTiO}_3$  (see below). The appropriate cubic PNS would be the  $P^*$  surface, which is very close to the well known Schwarz's  $P$  minimal surface. The PNS  $P^*$  is generated by  $|S(100)| = |S(010)| = |S(001)| = 1$  and  $\alpha(100) = \alpha(010) = \alpha(001) = 0$  and may be symbolized by  $Pm\bar{3}m \langle (100)_0^1 \rangle Im\bar{3}m$  according to [2]<sup>1</sup>. The corresponding coefficients in the  $I4/mcm$  setting are  $|S'(002)| = 1.0$  with  $\alpha(002) = \pi$  and  $|S'(110)| = 0.83$  with  $\alpha(110) = 0$ . The phase shift  $\alpha(002)$  regards the different origins of  $I4/mcm$  and  $Pm\bar{3}m$ . The relative values of the decay function  $k_{\mathbf{h}} \sim |\mathbf{h}|^2$  reflect the axial ratio  $c/a$ . They are normalized to that of the shortest  $h$  vector ( $k(002) = 1$ ) and included in the coefficients  $S'_h = S_h \cdot k_{\mathbf{h}}$ .

This modified PNS  $I4/mcm \langle (002)_0^1 (110)_{\pi}^{0.83} \rangle I4/mcm$  is shown in Fig. 1(a) and Fig. 1(b):

(a) The PNS looks very similar to the PNS  $P^*$  but has smaller necks along  $[001]$ , which results from the larger weight of  $|S'(002)|$ . The space is divided into two identical labyrinths. One of them (light blue) contains the polyhedral network and the other (dark blue) seems to be "empty".

(b) In this representation, the  $\text{PdGa}_5$  structure is a hierarchical derivative of the perovskite structure ( $\text{CaTiO}_3$ ). The polyhedral  $[\text{PdGa}_{10/2}]$  network plays the role of the  $[\text{TiO}_{6/2}]$  frame and the Ca position is not occupied.

(c) The PNS also divides the space into the regions of different chemical interactions. The "empty" space is the region of highest electron localization (see Fig. 1(e) and further discussion).

## 4. Bonding

### 4.1. Quantum mechanical procedure

The electronic structure of  $\text{PdGa}_5$  was calculated by use of the local density functional approach (LDA) with the exchange correlation potential of Barth and Hedin [6] as implemented in the tight binding LMTO program package of Krier et al. [7]. The radial scalar-relativistic Dirac equation was solved to get the partial waves. The calculation within the atomic spheres approximation (ASA) includes corrections for the neglect of the interstitial regions and the partial waves of higher order [8]. Interstitial spheres (E) had to be added to reduce the overlap of the atomic spheres (radii:  $r(\text{Pd}) = 1.437 \text{ \AA}$ ,  $r(\text{Ga1}) = 1.585 \text{ \AA}$ ,  $r(\text{Ga2}) = 1.462 \text{ \AA}$ ,  $r(\text{E1}) = 0.752 \text{ \AA}$ ,  $r(\text{E2}) = 0.648 \text{ \AA}$ ).

The electron localization function (ELF) was evaluated according to [9]. In the density functional approach, this quantity depends on the local excess of kinetic energy density due to the Pauli principle (Pauli kinetic energy  $t_p(r)$ ) [10]. ELF is defined as  $\text{ELF} = \{1 + [t_p(r)/t_{p,h}(\rho(r))]^2\}^{-1}$ , where  $t_{p,h}(\rho(r))$  is  $t_p(r)$  of the homogeneous electron gas with the density  $\rho(r)$ . The ELF values are limited in the range  $0 < \text{ELF} \leq 1$  by this equation. High ELF values correspond to a low Pauli kinetic energy density, namely in regions of core shells, covalent bonds or lone pairs.

To get more insight into the structure of regions with higher localization, ELF can be analyzed using the procedure, proposed by Bader [11] for the electron density. Applying the theory of gradient vector fields, the whole ELF map can be divided into the basins of core attractors, bonding attractors and non-bonding attractors [12,13]. Integration of the electron density within these basins gives the number of electrons belonging to the according attractor [14]. The integration procedure used in this work is described in detail in [15]. For bonding attractors, this gives access to the bond multiplicity [16].

### 4.2. Band structure of $\text{PdGa}_5$

The calculated band structure of  $\text{PdGa}_5$  is shown in Fig. 2. The contributions of selected atomic orbitals are marked by "fat bands". The complicated pattern shows metallic character (no band gap found). The  $4p_z$ -orbitals of Ga2 and  $4d_{z^2}$ -orbitals of Pd contribute to distinct bands mainly along the  $\Gamma$ -Z- and  $P$ -X-directions (Fig. 2(a) and Fig. 2(b)). Ga1 atoms contribute in all regions of the band structure (Fig. 2(c)).

The calculated DOS patterns (Fig. 3) confirm these results. Both orbitals,  $4d$  of Pd and  $4p$  of Ga2 have maxima of DOS in the region between  $-3$  and  $-5 \text{ eV}$  (Fig. 3(a) and Fig. 3(b)). The density of states for  $4s$  and  $4p$  orbitals of Ga1 does not reveal any pronounced maxima over the whole region calculated (Fig. 3(c)).

<sup>1</sup>The symbol starts with the generating space group symmetry, followed by brackets  $\langle \rangle$  and ends with the resulting PNS space group symmetry. The brackets  $\langle \rangle$  contain the informations about the representative Fourier coefficients  $(hkl)_\alpha^{|S|}$ . The complete set of Fourier coefficients which are symmetry related with the representative  $(hkl)_\alpha^{|S|}$  has to be used in the Fourier series. This set is derived by permutation of  $hkl$  and  $\alpha$  according to the generating space group symmetry.

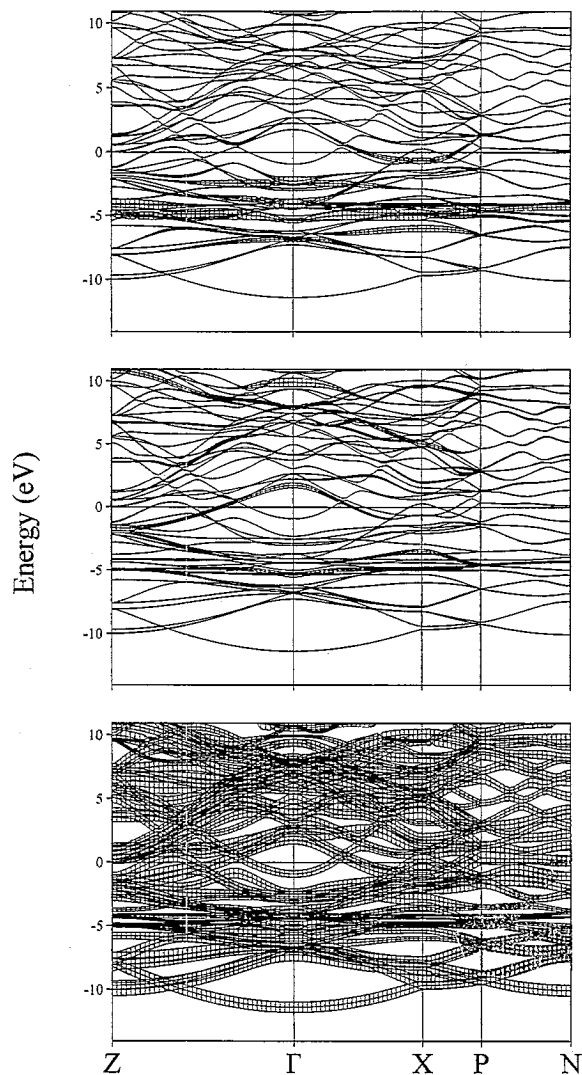


Fig. 2. Band structure of PdGa<sub>5</sub>: fat band representation of Pd 4d<sub>2</sub> (a), Ga2 4p<sub>z</sub> (b) and Ga1 4s+4p (c) orbitals.

No conclusions about the kind of chemical interactions can be made in the structure of PdGa<sub>5</sub> using this type of presentation for quantum mechanical calculations.

#### 4.3. Electron density and ELF

The distribution of valence electrons is shown by the isosurface of electron density with  $\rho = 0.035 \text{ e}^-/\text{bohr}^3$  (Fig. 1(c)). There are clearly two different regions of high electron density, namely: (a) inside the PdGa<sub>10/2</sub> polyhedra representing the heteroatomic bonds and (b) between Ga1 atoms of different polyhedra representing the homoatomic bonds.

The electron density inside the polyhedra is mainly formed by the 4d-orbitals of palladium and 4s- and 4p<sub>z</sub>-orbitals of Ga2 as well as the 4s- and 4p-orbitals of Ga1. The 4p<sub>x</sub>- and 4p<sub>y</sub>-orbitals of Ga2 are practically not

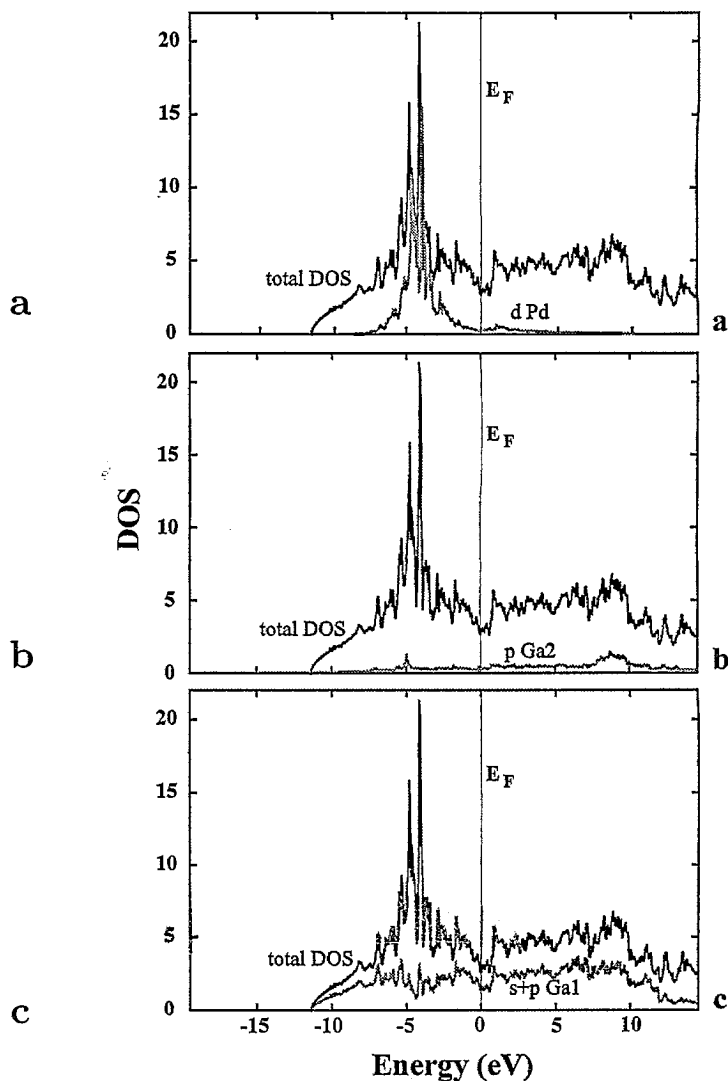


Fig. 3. Density of states for palladium 4d (a), Ga2 4p (b) and Ga1 4s+4p (c) orbitals in comparison with total DOS of the PdGa<sub>5</sub> compound. DOS values correspond to all atoms of each type in the unit cell (2Pd, 8Ga1 and 2Ga2).

involved in the occupied bands in this region. The electron density in the second region (between the polyhedra) is formed by all Ga1-orbitals (including 4p<sub>x</sub> and 4p<sub>y</sub>).

The ELF calculations classify the two regions of high valence electron density as regions with complete different character. High valence ELF values ( $\text{ELF} > 0.65$ ) are positioned between four Ga1 atoms of different antiprisms (Fig. 1(d)) in the "empty" labyrinth (Fig. 1(e)). In contrast to these regions of homoatomic Ga1–Ga1 bonds, the ELF values inside the PdGa<sub>10/2</sub> polyhedra are low in general, except a small region around the Ga2 atoms of the Pd–Ga2 chains along [001]. Obviously, these infinite chains as well as the (Ga1)<sub>4</sub> squares play an important role in the organization of the PdGa<sub>5</sub> structure (Fig. 1(f)). The (Ga1)<sub>4</sub> squares are arranged in staggered configuration along the two-fold [110] axis and along the four-fold [001] axis.

Trigonal prisms and tetrahedra of Ga1 atoms result by this arrangement, but these fragments are “open” and not covalently bonded structural units (Fig. 1(f)).

The high ELF maxima at the centers of the Ga1–Ga1 bonds allow the definition of bonding attractors. The number of valence electrons were integrated for each ELF attractor basin (Section 4.1). One obtains 1.2 electrons for the Ga1–Ga1 bond attractor basin parallel to the (001) plane and 0.8 electrons for the Ga1–Ga1 bond attractor basin parallel to the [001] axis. Thus the average bond order of each of the four Ga–Ga bonds in the (Ga1)<sub>4</sub> square is  $s=1/2$ , in other words, each Ga1 atom spends one electron to form the (Ga1)<sub>4</sub> square.

In order to check the validity of the use of valence ELF for bonding interpretation in PdGa<sub>5</sub>, we performed additional calculations including the 3d-orbitals of gallium into the valence shell. As stated in [17], this should lead to an overall decrease of ELF. In fact, for PdGa<sub>5</sub> the maximum value of ELF decreases from 0.84 for the usual choice of valence orbitals to 0.48 when including 3d-orbitals of gallium. However, the topology of ELF does not change significantly, especially in the regions of highest localization. Thus, the integrated electron density in the Ga1–Ga1 bond attractors remains practically the same.

## 5. Conclusion

The PdGa<sub>5</sub> structure is hard to understand by the classical description in terms of PdGa<sub>10</sub> polyhedra. Quantum chemical calculation gives a new insight into the fundamental bonding elements in intermetallic compounds of this type. Two main regions with different qualities in chemical bonding can be identified by the analysis of the valence electron density and the electron localization function. These regions are separated by the appropriate periodic nodal surface.

Four of the five Ga atoms form homoatomic bonds with a relative high degree of covalency. This results in the formation of slightly stretched Ga<sub>4</sub> squares formed by Ga1 atoms of different PdGa<sub>10</sub> polyhedra. These squares are bonded by four valence electrons (1 e<sup>-</sup>/Ga) and can be described as half bonded Ga<sub>4</sub> squares or as an average resonance structure formed by two single-bonded Ga<sub>2</sub> pairs.

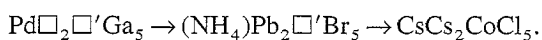
It seems that the interatomic Ga–Ga distances are not a good measure for the covalent bonding interactions. At the periphery of the PdGa<sub>10</sub> polyhedra, Ga–Ga distances exist of about 2.828, 2.898 or 2.903 Å, which are not substantially larger than the bond distances in the Ga<sub>4</sub> square (2.669 and 2.787 Å).

Inside the polyhedra, the electrons are mostly delocalized. Two different types of gallium atoms are present: one type form the covalent Ga<sub>4</sub> groups, the other type is involved in the more metallic interaction with palladium

along [001]. The whole structure of PdGa<sub>5</sub> can be described as a framework of one-dimensional microscopic wires in a covalent gallium matrix. This may possibly lead to an anisotropy of the electrical conductivity.

According to this description, the electrical conductivity is that of metals like Ga or Pb (specific resistance  $\rho=20 \times 10^{-6} \Omega \text{ cm}$ ). The magnetic susceptibility  $\chi_{\text{mol}}$  ranges from  $-30 \times 10^{-6} \text{ cm}^3 \text{ mol}^{-1}$  at 4 K to  $-71 \times 10^{-6} \text{ cm}^3 \text{ mol}^{-1}$  at 350 K, which corresponds to the presence of the Ga<sub>4</sub> squares (12 electrons) and Pd(d<sup>10</sup>) included in [Pd<sub>2</sub>Ga<sub>2</sub>] chains ( $2 \times d^{10} + 6$  electrons). No superconductivity was found above 2 K. The expected anisotropy of the electrical conductivity could not be measured up to now because of the lack of single crystals of appropriate size.

It can be shown, that the structures of the two ternary halides (NH<sub>4</sub>)Pb<sub>2</sub>Br<sub>5</sub> [18] and CsCs<sub>2</sub>CoCl<sub>5</sub> [19] can be described as stuffed derivatives of PdGa<sub>5</sub>:



The antiprismatic framework is build by the ions NH<sub>4</sub><sup>+</sup> and Br<sup>-</sup> or by Cs<sup>+</sup> and Cl<sup>-</sup>. The additional cations Pb<sup>2+</sup>, Co<sup>2+</sup> and Cs<sup>+</sup> compensate the charge of the framework and are located in the “empty” labyrinth of PdGa<sub>5</sub> structure.

Obviously these are more ionically bonded compounds, but nevertheless the same PNS separates regions of different strength of interaction, e.g., regions with larger and smaller coordination of the cations.

## References

- [1] Yu. Grin, U. Wedig and H.G. von Schnering, *11th Int. Conf. Solid Compounds of Transition Metals*, Abstracts, Wrocław, Poland, 1994, p. 39.
- [2] Yu. Grin, U. Wedig and H.G. von Schnering, *Vth Europ. Conf. Solid State Chem.*, Book of Abstracts, Vol. 2, Montpellier, France, 1995, p. 490.
- [3] Yu. Grin, U. Wedig and H.G. von Schnering, *Angew. Chem.*, 107 (1995) 1318; *Angew. Chem. Int. Ed. Engl.*, 34 (1995) 1204.
- [4] Yu. Grin and H.G. von Schnering, *Z. Kristallogr.*, in press.
- [5] H.G. von Schnering and R. Nesper, *Z. Phys. B., Condensed Matter*, 83 (1991) 407.
- [6] U. Barth and L. Hedin, *J. Phys. C*, 5 (1972) 1629.
- [7] G. Krier, O. Jepsen, A. Burkhardt and O.K. Andersen, *The Program TB-LMTO-ASA*, Version 4.5, Max-Planck-Institut für Festkörperforschung, Stuttgart, 1995.
- [8] O.K. Andersen, Z. Pawłowska and O. Jepsen, *Phys. Rev. B*, 34 (1986) 5253.
- [9] A.D. Becke and K.E. Edgcombe, *J. Chem. Phys.*, 92 (1990) 5397; A. Savin, A.D. Becke, J. Flad, R. Nesper, H. Preuß and H.G. von Schnering, *Angew. Chem.*, 103 (1991) 421; *Angew. Chem. Int. Ed. Engl.*, 30 (1991) 409.
- [10] A. Savin, O. Jepsen, J. Flad, O.K. Andersen, H. Preuß and H.G. von Schnering, *Angew. Chem.*, 104 (1992) 186; *Angew. Chem. Int. Ed. Engl.*, 31 (1992) 187.
- [11] R.F.W. Bader, *Atoms in Molecules: A Quantum Theory*, Oxford Univ. Press, Oxford, 1990.
- [12] B. Silvi and A. Savin, *Nature*, 371 (1994) 683.
- [13] A. Savin, B. Silvi and F. Colonna, *Can. J. Chem.*, 74 (1996) 1088.

- [14] A. Savin, *2nd Int. Conf. Inorg. Chem., Stuttgart, 1993*.
- [15] F. Wagner, H.P. Beck and H.G. von Schnering, to be published.
- [16] U. Häusermann, S. Wengert and R. Nesper, *Angew. Chem.*, 106 (1994) 2150; *Angew. Chem. Int. Ed. Engl.*, 33 (1994) 2073.
- [17] M. Kohout and A. Savin, *J. Comp. Chem.*, in press.
- [18] H.M. Powell and H.S. Tasker, *J. Chem. Soc. London*, (1937) 119.
- [19] P.A. Reynolds, B.N. Figgis and A.H. White, *Acta Crystallogr. B*, 31 (1981) 508.